Permeation of Water Vapor Through Cellulose Triacetate Membranes in Hollow Fiber Form

C. Y. PAN, C. D. JENSEN, C. BIELECH, and H. W. HABGOOD, *Alberta Research Council, Edmonton, Alberta T6G 2C2, Canada*

Synopsis

A modification of the carrier gas method for measuring permeability of a hollow fiber to a vapor is described with particular application to water vapor permeation through asymmetric cellulose triacetate in hollow fiber form. Conventional methods are inadequate because the high flux of permeation vapor combined with its low pressure on the permeate side and the small diameter of the fiber lead to an excessive buildup of pressure in the permeate stream—in some cases so great as to render much of the fiber length ineffective. The method described in this paper involves the permeation from the outside to the inside of the fiber of a binary mixture consisting of the water vapor and a fairly highly permeable carrier (helium). There is a significant pressure drop along the fiber, but a theoretical treatment is presented to take this into account and to permit a determination of the vapor permeability. Experiments at 35°C over a range of water vapor pressures up to 1.7 cm Hg gave a water flux of 9×10^{-3} cc(S.T.P.)/cm^2-sec-cm Hg, with an apparent slight decrease with increasing pressure. Over the same range of water vapor pressure the helium flux decreased from 2.3×10^{-4} to 1.85×10^{-4} cc(S.T.P.)/cm^2-sec-cm Hg.

INTRODUCTION

The principal objective of the work reported here was to measure the permeability to water vapor of cellulose triacetate membranes of the asymmetric or skin type when they are in the form of hollow fibers. This was an outgrowth of a larger program in these laboratories to develop a process for recovering helium from dilute concentrations in natural gas using a permeation technique. Water vapor is a minor component of most gas streams; and since water permeates at a rate comparable to that of helium, it is important to be able to measure its permeability. It was difficult or impossible to use conventional methods for measuring the water vapor permeability of hollow-fiber membranes because of the effect of the pressure drop of gas flowing through the relatively small (~70 μm) internal diameter of the fibers. Accordingly, a modified method based on the binary permeation of a mixture of helium and water vapor has been developed.

The permeability of a gas or vapor through a flat membrane is usually determined by measuring the permeate flux under a known uniform pressure differential across the membrane sample. This can also be done in the presence of a carrier gas on both sides of the membrane as proposed by Ziegel et al.[1,2] In this instance, the carrier gas flows are maintained high enough to ensure a uniform feed-side partial pressure of the permeating component and a negligible permeate-side partial pressure relative to that in the feed side. In the case of highly permeable hollow fine fibers, such as the H_2O–CTA hollow fiber system studied here (fiber I.D. 70 μm, O.D. 225 μm, and Q/d 9×10^{-3} cc(S.T.P.)/cm^2-sec-cm Hg), the conventional methods cannot be used mainly because of the significant

Journal of Applied Polymer Science, Vol. 22, 2307–2323 (1978)

0021-8995/78/0022-2307$01.00

permeate pressure buildup inside the fiber (or feed pressure drop if the feed flows inside the fiber).

This is a particularly serious problem for the water vapor system because the experiments are restricted to low vapor pressures, which mean correspondingly high volumetric flow rates and hence high pressure drops. For example, the water permeate flow generated by a 1.0-cm Hg vapor pressure differential across a membrane surface corresponding to a 1-cm length of the fiber studied here is expected to be around 6×10^{-4} cc(S.T.P.)/sec. But the pressure drop for such a flow through a fiber of 1-cm length and 70-μm I.D. would be 2.4 cm Hg if the permeate outlet pressure is maintained at 1.0 cm Hg. Obviously, then, it would be impossible to maintain a uniform pressure differential across any appreciable area of membrane surface. It would also be difficult to measure the pressure difference from one end to the other and then to calculate a permeability from the varying differential driving force.

The Ziegel (carrier gas) method would require a high gas flow inside the fiber to maintain a near-uniform partial pressure of water, and this is the case whether the feed is inside or outside. If the feed is inside, the pressure gradient along the fiber will cause a decrease in partial pressure of the water even if the mole fraction can be maintained relatively constant. If the permeate is inside, the carrier flow necessary to maintain a near-uniform low partial pressure will be prohibitive, e.g., a few hundred psi pressure drop through a 14-cm length of fiber could easily be required to keep the permeate partial pressure less than 10% of the feed partial pressure.

Because of these problems with conventional methods, we have developed a method that in some respects is a modification of the carrier gas technique.

Basically, the permeability of water vapor through the CTA hollow fiber is determined by studying the permeation of a water vapor and helium mixture. In essence, the water vapor permeability is measured through the relative permeation rates of water and helium. Figure 1(c) shows such a permeation system at a steady state [in comparison with the other two systems shown in (a) and (b)]. The feed flows outside the fiber and the permeate flows countercurrently inside of the fiber. The water partial pressure (and concentration) in the feed stream decreases along its flow path because the fiber is more permeable to water vapor than helium. There is a significant permeate pressure buildup inside the fiber, and the water partial pressure differential across the fiber varies significantly over the fiber length. The black dots in the diagram indicate the measurable points of flow rates and concentrations. The partial pressure of water inside the fiber cannot be measured directly but can be calculated in the course of solving the differential equations that describe the permeation system.

The other portions of Figure 1 illustrate in a similar manner the other two methods for measuring permeability. The conventional method using water vapor alone would end up with only a very short and indeterminate fraction of the fiber acting effectively. In addition, the measurement would require an elaborate vacuum system. The carrier gas method would be accompanied by extreme experimental difficulties because of the high gas flow rates and pressure drops to maintain the necessary near-constant partial pressures.

In this paper we develop the theory for the modified method of measuring gas permeabilities and report the results of a series of experiments. The theory describes the final steady-state situation as illustrated in Figure 1. Although

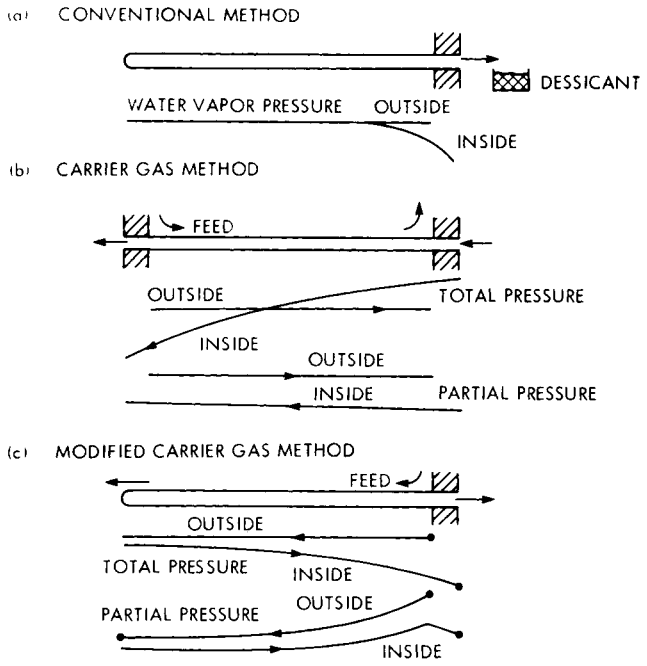

Fig. 1. Schematic illustration of the principles of three methods for measuring the permeability of hollow fibers to water vapor. (a) The hollow fiber is immersed in an atmosphere of water vapor and the permeate is collected from the inside of the fiber for a measured period by a desiccant and weighted. (b) Water vapor in helium flows over the outside of the fiber and helium is injected down the bore of the fiber as a carrier. The water content at the exit is monitored. For a 15-cm length of fiber a pressure difference of 25 atm from one end to the other must be maintained to ensure that the difference of water vapor pressure across the membrane does not vary by more than 10%. Both transient and steady-state data can be obtained. (c) Modified system used in the present work. A water–helium feed is used and the permeating helium serves as a carrier in the permeate stream. Lower helium flow rates and pressures can be used than in (b), and the full length of the fiber is effectively used rather than the small fraction which is active in (a). The method of iterative calculations used to solve (c) is described in the text.

the experiment can also record the transient approach to steady state, we have not been able to treat this theoretically.

THEORY

Steady-State Permeation into Hollow Fibers

The permeation of a binary gas mixture into the interior of a hollow fiber is shown schematically in Figure 2 and may be described by the following set of equations: The permeation at any point is given by

$$\frac{d(Vy)}{dl} = \pi D_0 \left(\frac{Q_2}{d}\right) (Px - py) \tag{1}$$

for water, and

$$\frac{d[V(1-y)]}{dl} = \pi D_0 \left(\frac{Q_1}{d}\right) [P(1-x) - p(1-y)] \tag{2}$$

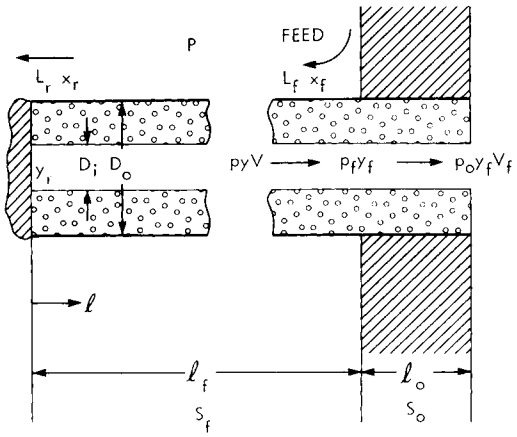

Fig. 2. Countercurrent permeation in hollow fiber. Schematic to illustrate nomenclature used in equations.

for helium, where x and y are the mole fractions in the feed-side and permeate-side streams, V is the permeate-side flow rate in cc(S.T.P.)/sec, P and p are the feed- and permeate-side pressures in cm Hg, D_0 is the outside diameter of the fiber in cm, l is the distance from the closed end of the fiber in cm, and Q/d is the permeation flux in cc(S.T.P.)/cm^2-sec-cm Hg. Because the effective thickness of the permeation skin d is not directly measurable, it is more convenient to deal with the permeation flux Q/d rather than with the permeability Q. Since Q always occurs along with d in this ratio, this has no effect on the theoretical development.

The pressure drop due to flow of permeate along the inside of the fiber (inside diameter D_i in cm) is given by

$$\frac{dp^2}{dl} = \frac{-256RTV\mu}{\pi g_c D_i^4} \tag{3}$$

where the temperature T, viscosity μ, gas constant R, and Newton's law conversion factor g_c are all in consistent units. Finally, the material balance for the countercurrent flow pattern of Figure 2, taken from the closed end to any point along the fiber, is given by

$$L = L_r + V \tag{4}$$

$$Lx = L_r x_r + Vy \tag{5}$$

where L is the feed-side flow rate and the subscript r refers to the residue (closed fiber end).

These equations are subject to the following assumptions:

(1) The permeability of each gas component is independent of pressure and concentration.

(2) Negligible gas-phase concentration gradients in the permeation direction.

(3) Diffusion along the flow path is insignificant compared to the bulk flow.

(4) Feed gas flows outside of the fiber with negligible pressure drop.

(5) The permeate flow inside the fiber is governed by the Hagen-Poiseuille equation, i.e., eq. (3).

(6) The viscosity of the permeate is assumed to be independent of pressure and to vary with composition according to $\mu = \mu_2 y + \mu_1(1 - y)$.

(7) The fiber is of the asymmetric type with a thin active layer on the outside of the fiber. For a symmetric fiber, D_0 in the above equations must be replaced with the logarithmic mean diameter $(D_0 - D_i)/\ln(D_0/D_i)$.

These assumptions are reasonable and straightforward except, perhaps, assumptions (1) and (5). The water permeability may vary with the vapor pressure, and the helium permeability may be affected by the presence of water in the membrane, but the variation of these permeabilities over the length of the fiber for any given set of experiments may be minimized by reducing the vapor pressure difference in the feed and residue streams. With respect to assumption (5), eq. (3) applies, strictly speaking, only to laminar flow in an impermeable tube. Berman[3] has obtained a solution for the pressure profile of a laminar flow stream in a channel with porous walls, and it can be shown that his solution reduces to the integrated form of eq. (3) (taking into account the flow variation) provided only that the "permeation Reynolds" number, defined as D_i(permeate flux)/μ, is much less than 1. For the system studied here, the permeation Reynolds number is in the order of 10^{-5}, and assumption (5) is justified.

Formulation. The above equations may be reformulated for more convenient solution. From eqs. (4) and (5) we obtain

$$L/L_r = (y - x_r)/(y - x) \tag{6}$$

$$V/L_r = (x - x_r)/(y - x) \tag{7}$$

Substituting eq. (7) into eqs. (1) and (2) and then solving for dy/dx and dS/dx from the resulting equations yields

$$\frac{dy}{dx} = \frac{y - x_r}{x - x_r}\left\{\frac{\alpha(1 - y)(x - \gamma y) - y\,[1 - x - \gamma(1 - y)]}{\alpha(1 - x)(x - \gamma y) - x[1 - x - \gamma(1 - y)]}\right\} \tag{8}$$

$$\frac{dS}{dx} = \frac{(x_r - y)/(x - y)}{\alpha(1 - x)(x - \gamma y) - x[1 - x - \gamma(1 - y)]} \tag{9}$$

where $\alpha = Q_2/Q_1$, $\gamma = p/P$, and $S = (Q_1/d)(P/L_r)\pi D_0 l$. With the aid of eq. (7), eq. (3) may be written as

$$\frac{d\gamma^2}{dS} = \frac{\psi[\mu/\mu_1]\,(x - x_r)}{S_f{}^2(x - y)} \tag{10}$$

where

$$\psi = 256\mu_1 RTD_0(Q_1/d)l_f^2/g_c P D_i^4 \tag{11}$$

$$S_f = (Q_1/d)(P/L_r)\pi D_0 l_f \tag{12}$$

μ_1 is the viscosity of helium and l_f is the active fiber length. Over the inactive fiber length imbedded in the tube sheet, (cf. Fig. 2) eq. (10) yields

$$\gamma_f^2 = \gamma_0^2 + \frac{\psi[\mu/\mu_1]\,(x_f - x_r)}{(l_f/l_0)S_f(y_f - x_f)} \tag{13}$$

where the subscript 0 refers to the permeate outlet. Thus, the equations governing the permeation system become eqs. (6)–(10).

The boundary values of y_r and $(dy/dx)_r$ at the residue end require special

attention and will now be noted. y_r is a known function of x_r and is determined through the relation that $y_r/(1 - y_r)$ is equal to the ratio of the right-hand sides of eqs. (1) and (2).[4] This gives

$$y_r = \frac{2\alpha x_r}{1 + (\alpha - 1)(x_r + \gamma) + \sqrt{[1 + (\alpha - 1)(x_r + \gamma)]^2 - 4\gamma\alpha(\alpha - 1)x_r}} \quad (14)$$

The corresponding value of eq. (8), which appears indeterminate with y_r given by eq. (14), can be determined by L'Hopital's rule[4] and is given by

$$\left(\frac{dy}{dx}\right)_r = \frac{(y_r - x_r)\,[\alpha - (\alpha - 1)y_r]}{\alpha(1 - x_r)(x_r - \gamma y_r) - x_r[1 - x_r - \gamma(1 - y_r)] - (y_r - x_r)} \times [(\alpha - 1)(2\gamma y_r - x_r - \gamma) - 1] \quad (15)$$

Method of Solution. Considering now an actual experimental system such as illustrated in Figure 2, we outline the general method of solution. The fiber lengths, active and inactive (l_f and l_0), are fixed and known, as are the feed pressure P and the permeate outlet pressure p_0. There are three flow rates and three compositions (feed, residue, and permeate), L_f, L_r, V_f, x_f, x_r, and y_f, that may be measured, but those are related by the two material balance equations, eqs. (6) and (7), so that only four are truly independent. From these four independent measurable quantities we want to determine the two permeabilities Q_1 and Q_2 by means of the remaining three equations, eqs. (8)–(10). Of these three equations, however, eq. (10) exists only to provide values for the permeate pressure along the fiber to be inserted into eqs. (8) and (9), so that in effect we are left with two unknowns to be determined from two equations. There remains the additional problem, however, which four of the six measurable quantities to choose since for practical reasons there will be some error in the material balance. This matter will be discussed under Results.

Coming to the specific method of solution, it has not been possible to obtain an analytical solution of eqs. (6)–(10). Consequently, we have determined Q_1 and Q_2 by numerical solution using a trial-and-error procedure. In this procedure, values are assumed for Q_1 and Q_2 and only two of the four measured concentrations and flows are needed to obtain the solution of eqs. (6) to (10). If Q_1 and Q_2 have been correctly assumed, this solution will match the other two measured concentrations and flows, otherwise the procedure must be repeated with a new set of Q_1 and Q_2. The initial estimation of Q_1 (helium) is usually helped by a knowledge of the permeability to pure helium or by an approximate treatment in which the presence of water is initially ignored and a Q_1 is calculated from the observed permeate flow (see below).

In this calculation procedure the choice of the two measured concentrations and flows to be used as boundary conditions will affect the choice of computational method for obtaining the solution of eqs. (6)–(10). We have found that the computational effort is minimized if x_f and x_r are chosen and an iterative procedure is employed. If x_f and x_r have not been directly measured, they can be calculated from the other four measured quantities by the material balance equations.

Estimation of Q_1. Under the conditions of low water content in the feed and

permeate streams, the helium permeability can be calculated from the observed permeate flow V_f by eqs. (2) and (3) (with $x = y = 0$) as follows. [If V_f was not measured directly it can be calculated from other measured flows and concentrations via the material balance eqs. (6) and (7)]. Equation (3) can be readily integrated over the inactive length l_0 to give

$$p_f^2 - p_0^2 = \frac{256\mu RTV_f l_0}{\pi g_c D_i^4} \tag{16}$$

Dividing eq. (2) by eq. (3) and then integrating the resulting equation over the active length of the fiber yields

$$3P(p^2 - p_f^2) - 2(p^3 - p_f^3) = \frac{384\mu RT}{\pi^2 g_c D_i^4 D_0 (Q_1/d)}(V_f^2 - V^2) \tag{17}$$

This p–V relation can be used to integrate eq. (2) or (3). However, it is important to note that eq. (3) gives rise to an improper integral with a singularity at $l = 0$ ($V = 0$). Such an integral cannot be evaluated numerically. Thus, it is more convenient to work with eq. (2), which may be written as

$$D_0(Q_1/d) = \frac{1}{\pi l_f}\int_0^{V_f} \frac{dV}{P - p} \tag{18}$$

The following iteration method may be used to determine Q_1/d: (1) Calculate the permeate pressure p_f, at the junction of the active and inactive fiber lengths by eq. (16). (2) As a first approximation, assume the permeate pressure at the closed end of the fiber, p_r, to be equal to $(P + p_f)/2$. Calculate the corresponding Q_1/d by eq. (17) (note that $p = p_r$, $V = 0$). (3) Calculate a new Q_1/d by numerically integrating the right-hand side of eq. (18) with the aid of eq. (17), in which the previously calculated Q_1/d is used. (4) Repeat step (3) until the value of Q_1/d converges to the desired accuracy. Normally 1% accuracy can be obtained within 10 iterations.

It is perhaps worth noting that the procedure described in this section to estimate the helium or carrier gas permeability can also be used with the method of Figure 1(a), which does not involve a carrier gas. As pointed out in the introduction, however, the calculations would not be very accurate for water vapor because the permeate pressure would almost equal the feed pressure over much of the length of the fiber.

Solution of Eqs. (6) to (10). With the experimental values of x_f and x_r, the value of Q_1 determined by the procedure described above, and an assumed Q_2, the solution of eqs. (8)–(10) can be obtained by an iterative calculation method. The iterative procedure starts with an assumed pressure profile from which a profile of the permeate concentration is generated by eqs. (8) and (9). This, in turn, is used to generate a new pressure profile by eq. (10). The advantage of this procedure is that eqs. (8)–(10) are integrated separately. The algorithm for this iteration method is described as follows: (1) As a first approximation, assume the permeate pressure to be independent of x and the γ to be everywhere equal to γ_0 (i.e., assume negligible permeate pressure drop). (2) With the aid of this x,γ relation, integrate eq. (8) numerically (preferable by the second-order Runga-Kutta method) from x_r to x_f to obtain the x,y relation and y_f. This relation is, in turn, used to integrate eq. (9) to yield the x,S relation (and hence x,y,S relation) and the value of S_f (corresponding to $x = x_f$). (3) Obtain a new

x,γ relation through the γ,S relation calculated by integrating eq. (10) from $S = S_f + S_0$ (where $\gamma = \gamma_0$) to $S = 0$, with the aid of the x,y,S relation obtained in step (2). (4) Repeat steps (2) and (3) until y_f converges to the desired accuracy, then calculate L_r, L_f, and V_f by eqs. (12), (6), and (7), respectively. This completes the calculation. Generally, 0.5% accuracy for y_f can be obtained within four iterations.*

Trial-and-Error Determination of Q. The solution achieved above will include, in addition to x_f and x_r, the remaining four concentrations and flows y_f, V_f, L_f, and L_r. These may be compared with the experimentally measured values. In making the comparison it must be remembered that because of the material balance restrictions, only four of the six quantities are independent. Furthermore, the estimation of Q_1 was based on the experimentally determined V_f, so it is to be expected that the calculated V_f will come close to matching the experimental value. Thus, we are left, in effect, with the need to match only one of the three remaining quantities (y_f, L_f, and L_r) as a criterion of proper choice of Q_2. In all three cases, if the calculated quantity is lower than the experimental quantity, the value chosen for the next trial should be increased. This is obvious in the case of y_f, less so for the other two.

When a reasonable match has been obtained here by adjustment of Q_2, the match of V_f may be reexamined and the value Q_1 adjusted for improved fit. This will require some further adjustment of Q_2. These last steps were not considered necessary in the work reported in this paper.

EXPERIMENTAL

Samples of Dow cellulose triacetate hollow fiber (kindly provided by L. J. Underhill of Dow Chemical USA, Walnut Creek, California) used in the permeation experiments were dried by solvent exchange with isopropanol and heptane.[5] Their apparent dimensions after drying were 225 μm O.D. and 70 μm I.D. The dense layer is on the outside, and the helium flux ($Q/d = 2.3 \times 10^{-4}$cc(S.T.P.)/cm^2-sec-cm Hg) and He/CH_4 selectivity (~77) indicated that substantially all of the asymmetric structure had been retained on drying.

A sample of symmetric film for comparison in sorption experiments was prepared by dissolving oven-dried cellulose triacetate fibers in dichloromethane and casting the solution onto a glass plate. The film used was 3 cm by 5.5 cm and had an average thickness of 260 μm and a weight of 560 mg.

The permeation apparatus, as shown in Figure 3, was set up such that a flow of dry helium at a constant pressure could be equilibrated with various partial pressures of water vapor in a saturator and then allowed to flow over the outside of a bundle of CTA hollow fibers. The saturator consisted of a 20-cm length of 1/2-in. tubing filled with crushed firebrick loaded with liquid water and kept at constant temperature.

The hollow fiber bundle consisted of 32 fibers of 14 cm active length. One end of the fiber bundle was sealed shut with epoxy resin and the other was potted through a 3-cm 1/4-in. copper tube with epoxy resin. The total surface area of the bundle was 32 cm^2. The fiber temperature was maintained at 35°C by means of a water bath.

* The computer programs, in Fortran language, are available from Alberta Helium Ltd., Box 1496, Calgary, Alberta.

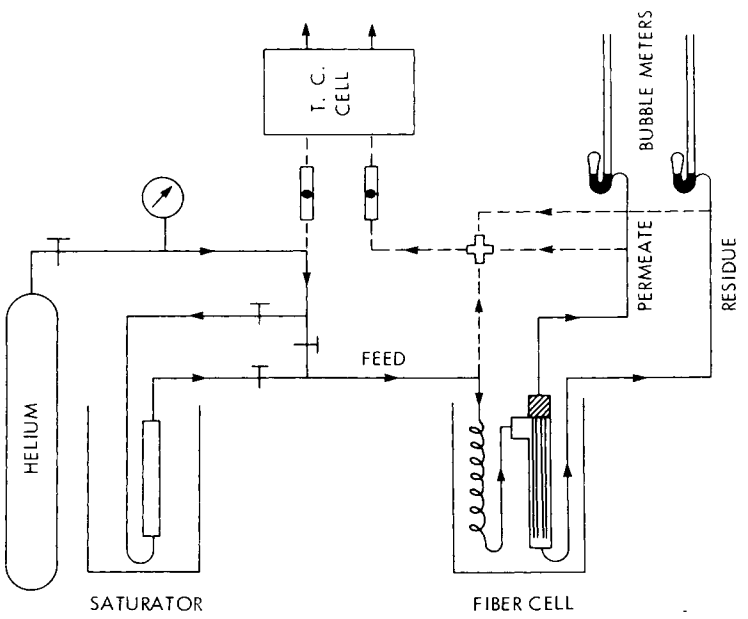

Fig. 3. Experimental apparatus. Bundle of fibers is mounted in cell in manner illustrated in Figure 2.

A Gow-Mac hot-wire thermal conductivity cell (W2X) connected to a Hewlett-Packard strip-chart recorder was used to measure the water content in the feed, residue, and permeate streams sequentially after the permeation system had reached the steady state. The calibration of the thermal conductivity cell was based on the concentration of water in the feed stream, assuming complete saturation at the temperature of the saturator. A stable calibration factor was obtained when the cell current (150 mA) and temperature were maintained constant. The rates of permeate and residue flows were measured by soap bubble meters with no correction for water vapor. The accuracies for the flow and concentration measurements were estimated to be within ±3%.

Sorption experiments were done in a conventional manner using a Cahn RG electrobalance in a vacuum mounting. The results reported in this paper are limited to rate measurements on the sample of symmetric film along with equilibrium (solubility) measurements on that and other samples. A number of only partially successful attempts were made to follow the sorption of water vapor by the hollow fibers, but it was difficult to obtain reliable and reproducible data during the very rapid early stages since about 80% of the total uptake occurs during the first minute. Some success was obtained by introducing the water vapor from a 5-liter reservoir which had been temporarily preequilibrated to a higher pressure such that after expansion into the 6-l. volume of the microbalance proper the desired pressure would be obtained. Nevertheless, there remained sufficient uncertainties in the experimental procedure that the data on hollow fibers were not considered reliable, and hence they are not given.

RESULTS

Figure 4 shows the recorder trace of a typical run with the transient buildup of the water concentration in the permeate stream and the steady-state concentrations in the feed and residue streams. The concentrations could be converted to partial pressures using the measured total pressures. The transient curve appears qualitatively similar to curves reported for the carrier-gas method but, as mentioned earlier, it would be expected to have significant quantitative differences.

A typical set of measurements and the calculated results are shown in Table I. The measured data are the residue and permeate flow rates (it was not convenient to measure the feed flow rate independently), the mole fraction of water vapor in the feed (calculated on the assumption of complete saturation in the saturator), and the mole fractions in the residue and permeate. From the flow rates and compositions, a water material balance was calculated as shown in the table. The 3% apparent loss is relatively high for the experiments performed. The helium permeation flux Q_1/d was next calculated from the observed per-

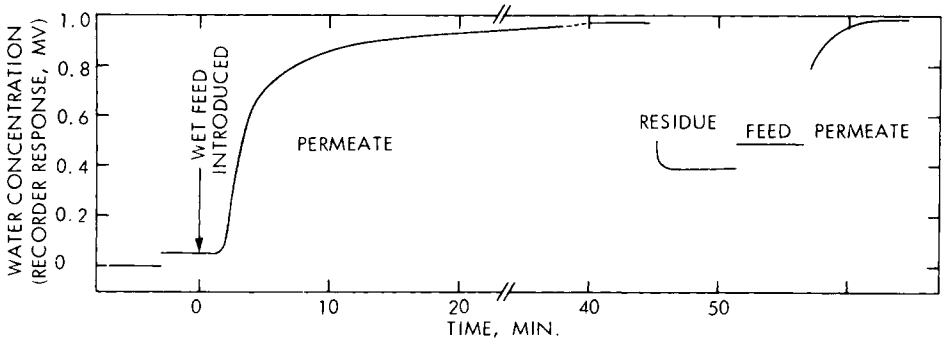

Fig. 4. Recorder trace (a measure of the mole fraction of water vapor) of a typical run showing the transient buildup of the water concentration in the permeate stream and the steady-state concentrations in the residue and feed streams. The small positive value at the beginning of the permeate curve is believed to indicate residual traces of water in the membrane.

TABLE I
Typical Permeation Experiment[a]

Measured Values							
Compositions	Mol fraction × 10^3	x_f	4.37[b]	x_r	3.48	y_f	8.80
Flows	cc(STP)/sec	V_f	0.46	L_r	2.77		
Water Balance							
In:		4.37(2.77 + 0.46) = 14.11					
Out:		3.48 × 2.77 + 8.80 × 0.46 = 13.69					
Out/in:		0.97					
Q_1/d Calculated by Matching V_f, 1.89 × 10^{-4} cc(S.T.P.)/cm²-sec-cm Hg							
Q_2/d Calculation							
Data used for calculation				Calculated values			
x_f	x_r	y_f		V_f	2.29	Q_2/d	85.1 × 10^{-4}
x_f	y_f	V_f		x_r	3.63		75.6 × 10^{-4}
x_r	y_f	L_r		x_f	4.24		189 × 10^{-4}
x_f	x_r	L_r		y_f	[c]		[c]

[a] Fiber temperature 34.8°C.

[b] Based on feed pressure 33.2 psia, saturator temperature 7.0°C.

[c] No solution was possible.

meate flow rate by the approximation given in the theoretical section. The value 1.89×10^{-4} is a little lower than 2.3×10^{-4} obtained for dry helium.

The water permeation flux Q_2/d can be calculated in four different ways using different combinations of the three concentrations and the residue flow rate. These values are shown in the body of the table along with the calculated value of the fourth parameter to compare with the observed value. There is, in this example, a wide spread among the Q/d values; runs with much closer material balance showed much smaller spread. Furthermore, it was found that starting with the observed values of x_f, x_r, and L_r, the governing differential equations could not generate any matching solution, i.e., convergence could not be obtained by the iterative calculation method used here. The reason for this is that these data, because of experimental inaccuracies, represent a physically impossible situation—the water vapor pressure in the permeate stream is apparently greater than that in the feed stream, which is reflected by the 3% material balance error.

The feed pressure in the permeation experiment should be chosen high enough that the ratio of feed pressure to permeate pressure is similar to the expected ratio of permeabilities of water to helium. This will ensure that the observed enrichment of water vapor in the permeate is determined primarily by the permeability ratio (which is the quality being studied in the experiment) rather than by the pressure ratio.[4] Once this requirement is met there is no advantage to having excessively high feed pressures. This feed pressure requirement was rather inadequately met in our experiments; a pressure of 33.5 psia was used, whereas a value closer to 200 psia would have been chosen on the basis of the results obtained. The use of the lower feed pressure made the calculated permeability values more sensitive to small errors in the measurements, and this is obvious in the results given later.

The feed-gas flow rate should be high enough to eliminate significant gas-phase mass-transfer resistances. This was tested by varying the flow rate to be sure that it had no effect on the permeability value.

Several experiments were carried out with a given feed composition and pressure but different feed flow rates. The results of one set of such experiments are summarized in Table II. The low flow rates correspond to low water permeabilities. This trend was consistently found in five separate sets of experiments. These results can be readily explained as being due to a channeling effect or major mass-transfer resistence occurring at flow rates below 1.5 cc/sec. The alternative explanation that the observed variation in calculated water permeability reflects a dependence upon water vapor pressure is ruled out by additional experiments over a range of water pressures at high flows which showed no such variation. Because of the flow dependence, subsequent data were all taken at flows greater than 1.5 cc/sec.

Table III summarizes the measurement of water fluxes in cellulose triacetate hollow fibers at 35°C over a pressure range up to 1.65 cm Hg. All of the possible calculated values of Q_2/d are given in the table. Three of the experiments had particularly good material balances, and these give Q_2/d values with relatively little variability. A best-fit straight line is drawn to the averages of these three experiments in Figure 5, which also includes the Q_2/d values from Table III. There is a suggestion of a slight drop in water vapor permeability with increasing partial pressure, but the results are inconclusive. Kawaguchi et al.[6] found a

TABLE II
Effect of Residue Flow

Residue flow, cc(S.T.P.)/sec	Vapor pressure, cm Hg		Material balance error, %	Permeation flux Q/d, 10^{-4}cc(S.T.P.)/sec-cm^2-cm Hg				
				Q_1/d calculated	Q_2/d Calculated by matching			
	Feed	Residue		by matching V_f	x_f, x_r, y_f	x_f, y_f, L_r	x_r, y_f, L_r	x_f, x_r, L_r
3.17	1.19	0.979	−2.9	1.85	83.0	83.0	185	
1.83	1.19	0.882	+0.2	1.84	82.9	82.9	82.9	73.7
0.69	1.19	0.487	−2.0	1.91	40.1	36.3	47.8	51.6
0.33	1.19	0.195	+1.8	1.98	29.7	37.6	27.7	25.7

TABLE III
Summary of Permeation Experiments—Water Vapor in CTA Hollow Fibers

Vapor pressure, cm Hg			Permeation flux Q/d, 10^{-4}cc(S.T.P.)/sec-cm^2-cm Hg					
			Q_1/d calculated	Q_2/d Calculated by matching				
Feed	Residue	Material balance error, %, 100(1-out/in)	by matching V_f	x_f, x_r, y_f	x_f, y_f, L_r	x_r, y_f, L_r	x_f, x_r, L_r	Average Q_2/d
0.48	0.340	+2.4	1.95	293	390	137	70.2	
0.48	0.405	+2.4	2.00	100	240	100	35.0	
0.751	0.564	+0.1	1.91	95.5	95.5	95.5	86.0	93.1
0.751	0.598	−3.0	1.89	85.1	75.6	246	—	
1.19	0.883	+0.2	1.84	82.9	82.9	82.9	73.7	80.6
1.19	0.979	−2.9	1.85	83.0	83.0	185	—	
1.65	1.23	+0.4	1.85	92.5	92.5	83.3	70.3	84.7
1.65	1.38	−2.4	1.83	82.4	82.4	183	—	
1.65	1.43	−6.0	1.72	86.0	77.4	—	—	

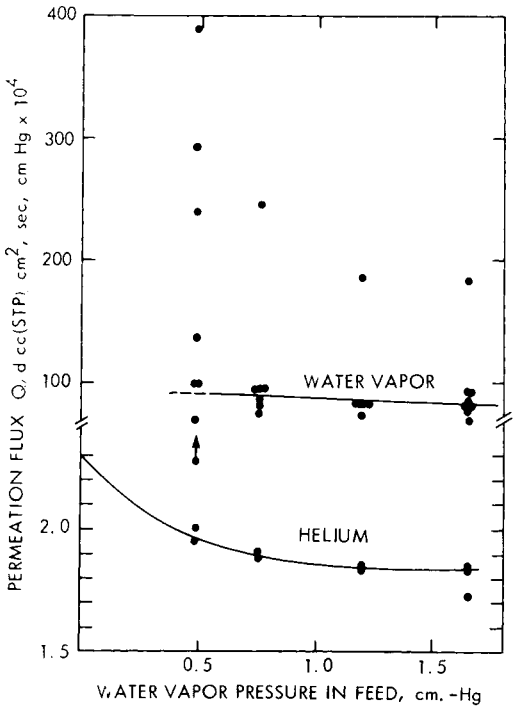

Fig. 5. Values of water vapor and helium flux for CTA hollow fibers, including line to fit averages of water vapor for three runs with least material balance error from Table III.

moderate increase in the permeability of symmetric CTA film with water vapor pressure.

The helium fluxes are also plotted in Figure 5; they decrease with increasing partial pressure of water vapor to an apparent limiting value. The data, however, are restricted to relative humidities of less than 40%, and it is possible that at high humidities, where the solubility coefficient of water increases, there may be a further decrease in the helium permeability. The effect of water vapor on the helium permeability of CTA is less than with the common cellulose acetate RO membrane.

The results described above are for the permeation flux Q/d through the asymmetric membrane of the hollow fiber. To obtain a value for Q, sorption experiments were done on the cast sample of symmetric film. From the rate curves, the diffusivity of water vapor at 35°C was determined to be 5×10^{-8} cm²/sec, with little concentration dependence over the 0%–50% R.H. range. From the equilibrium sorption, the solubility coefficient was found to be 20 cc(S.T.P.)/cc-cm Hg. These values give a permeability Q of 1.0×10^{-6} cc(S.T.P.)/cm-sec-cm Hg. This is a little lower than the literature values: 1.2×10^{-6} (26°) by Korvezee and Mol,[7] 1.5×10^{-6} (23°) by Kuo and McIntyre,[8] and 2×10^{-6} (25°) by Kawaguchi et al.[6] The first two of these were determined with one side of the membrane at 100% R.H., and the last covered a range of water vapor pressures on one side of the membrane and showed an increase in Q with relative pressure.

DISCUSSION

From the average value of water vapor flux Q/d for the hollow fibers and the value of the permeability Q obtained for the symmetric film we may calculate a value for the effective skin thickness d in the hollow fiber, which comes out to be 1.1 μm. Other estimates may be made on the basis of measurements of the fluxes of different gases as compared with permeabilities given in the literature, and these are summarized in Table IV. It is interesting that these other gases (He, N_2, O_2, and CH_4) all permeate with an apparent skin thickness of 0.04–0.06 μm. In other words, the skin thickness for water vapor is some 20 times that for the other gases. A similar range in variation in apparent skin thickness was also observed by Stern, Sen, and Rao[11] through the series O_2, N_2, Kr, and Xe in cellulose acetate films, with little obvious regularity.

The apparent skin thickness for water vapor is reasonably consistent with the "skin" as observed by the SEM (Fig. 6). This is similar to the conclusion of Lonsdale, Merton, and Riley[12] who, for standard flat-film CA membranes, deduced a skin thickness of 0.15 μm as compared with the 0.25 μm observed in electron microscope studies. Careful examination of the SEM image in Figure 6 shows a particularly dense layer of the "skin" at the outer surface, and this may be the active layer for the other gases which are less soluble in the cellulose triacetate.

In considering this method for the determination of gas permeabilities, several comments may be made. It is primarily suited to measuring the permeability of small-diameter asymmetric fibers to vapors or gases which are available only at low pressures, i.e., conditions where the conventional methods will give rise to an overwhelming permeate pressure buildup inside the fiber such as shown in Figure 1(a). If the gas is available at high pressure, the pure gas method [see Fig. 1(a)] may be used. The experiment would be done with a high permeate pressure and a relatively low feed–permeate driving pressure difference which would lead to a negligible permeate pressure buildup in the fiber. Alternatively, some pressure gradient in the fibers may be tolerated, provided a finite driving pressure is maintained over the full length of the fiber, and the method of solution based on eqs. (16)–(18) may be used. In the case of the carrier-gas method, Figure

TABLE IV
Effective Skin Thickness of CTA Hollow-Fiber Membrane

Permeate	CTA permeability Q, cc(S.T.P.)cm/ cm^2-sec-cm Hg	Temp., °C	CTA fiber flux Q/d, cc(S.T.P.)/ cm^2-sec-cm Hg	Temp., °C	Apparent skin thickness d, μm
H_2O (vapor)	1.0×10^{-6}	35	9×10^{-3}	35	1.1
He	1.36×10^{-9} [a]	22[9]	2.3×10^{-4}	35	0.06
N_2	1.7×10^{-11}	30[10]	4.2×10^{-6} [b]	24	0.04
O_2	1.0×10^{-10}	30[10]	1.6×10^{-5} [b]	24	0.06
CH_4	1.4×10^{-11}	22[9]	2.2×10^{-6}	24	0.06

[a] Data for cellulose acetate.

[b] Measured on a different bundle of CTA fibers; some samples may vary by up to a factor of 2.

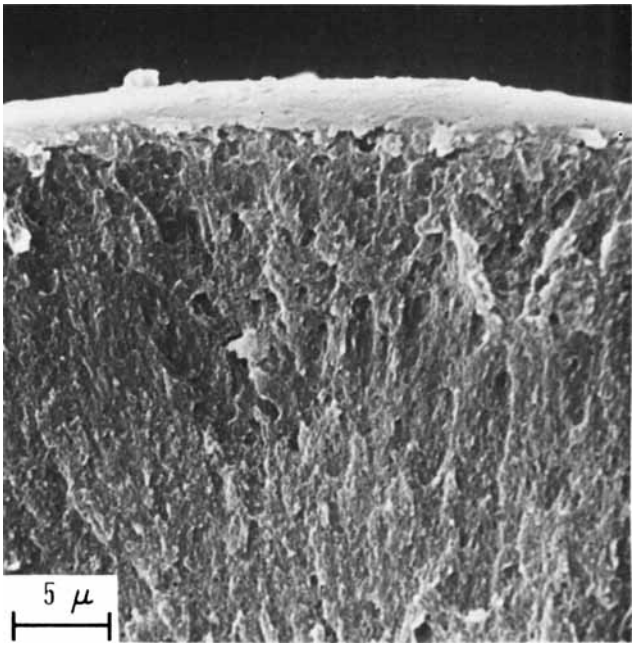

Fig. 6. Scanning electron microscope picture of a partial section of the asymmetric hollow fiber showing the skin layer.

1(b), measurements of hollow-fiber permeabilities are no easier for gases than for vapors.

There still remains the question of operating conditions when using this modified carrier gas method. It is possible that some combinations of carrier gas permeability, pressure, fiber diameter, and fiber length will lead to an inside pressure profile of the same qualitative shape as that shown in Figure 1(a); obviously, only an indeterminate fraction of the fiber is being measured, and this must be avoided. Then, in order to maintain a finite driving force for the carrier gas, a carrier gas of lower permeability may be required. On the other hand, the carrier permeability should not be too low because the permeability ratio (vapor/carrier gas) becomes higher and, as discussed earlier, a higher feed pressure is called for.

The authors wish to thank G. Braybrook of the University of Alberta for the SEM picture, M. M. Schurek for some technical assistance, and A. T. Blades for helpful discussion. Issued as Alberta Research Council Contribution No. 869.

References

1. K. D. Ziegel, H. K. Frensdorff, and D. E. Blair, *J. Polym. Sci. A-2,* **7,** 809 (1969).
2. D. G. Pye, H. H. Hoehn, and M. Panar, *J. Appl. Polym. Sci.,* **20,** 287 (1976).
3. A. S. Berman, *J. Appl. Phys.,* **24,** 1232 (1953).
4. C. Y. Pan and H. W. Habgood, *Ind. Eng. Chem., Fundam.,* **13,** 323 (1974).
5. W. R. MacDonald and C. Y. Pan, U.S. Pat. 3,842,515 (1974).
6. M. Kawaguchi, T. Taniguchi, K. Tochigi, and A. Takizawa, *J. Appl. Polym. Sci.,* **19,** 2515 (1975).

7. A. E. Korvezee and E. A. J. Mol, *J. Polym. Sci.*, **2**, 371 (1947).
8. J. F. Kuo and D. McIntyre, *J. Chinese Inst. Chem. Eng.*, **4**, 33 (1973).
9. P. K. Gantzel and U. Merten, *Ind. Eng. Chem., Proc. Des. Dev.*, **9**, 331 (1970).
10. S. T. Hwang, C. K. Choi, and K. Kammermeyer, *Separation Sci.*, **9**, 461 (1974).
11. S. A. Stern, S. K. Sen, and A. K. Rao, *J. Macromol. Sci.—Phys.*, **B10**(3), 507 (1974).
12. H. K. Lonsdale, U. Merten, and R. L. Riley, *J. Appl. Polym. Sci.*, **9**, 1341 (1965).

Received March 28, 1977